Desalination and Water Treatment
www.deswater.com

doi: 10.5004/dwt.2019.23320

138 (2019) 68–79
January

Preparation and characterization of PIM-1 and PIM-1/PU-blend membranes for pervaporation separation of phenol from water

Xiang Yan[a], Hong Ye[a,b,*], Chunxuan Dong[a], Yichen Wu[a], Shengpeng Shi[c]

[a]*Key Laboratory of Cleaner Production and Integrated Resource Utilization of China National Light Industry, Beijing Technology and Business University (BTBU), Beijing 100048, China, Tel./Fax: +86 10 68984307; emails: yehcn@163.com (H. Ye), 1073481046@qq.com (X. Yan), dcx951211@163.com (C. Dong), 18810528926@163.com (Y. Wu)*
[b]*Beijing Engineering and Technology Research Center of Food Additives, Beijing Technology and Business University (BTBU), Beijing 100048, China*
[c]*Beijing Research Institute of Chemical Industry, Beijing 100013, China, Tel. +86 10 59202781; email: sspcn@163.com*

Received 5 April 2018; Accepted 18 October 2018

ABSTRACT

Polymers of intrinsic microporosity (PIMs) are promising membrane materials for the recovery of phenol from water. In this study, PIM-1 and its blend membranes with polyurethane (PU) were prepared and characterized. The pervaporation separation performances of these membranes were evaluated using phenol aqueous solution. The result showed that PIM-1 with higher molecular weight led to better pervaporation separation performance. PU membrane modified with 1% PIM-1 exhibited pervaporation separation index (PSI), which higher than that of pristine PU and similar to that of pure PIM-1. Furthermore, addition of styrene–butadiene–styrene (SBS) as interfacial agent could improve the separation performance of blend membranes. When 0.125 wt% of SBS was added to 1% PIM-1/PU-blend membrane, both total flux and separation factor increased simultaneously from 14.6 to 16.1 kg μm m^{-2} h^{-1} and from 21.7 to 31.9, respectively, with 1% phenol in feed at 60°C. PSI of 1% PIM-1/PU with 0.125 wt% SBS is 498.1 kg μm m^{-2} h^{-1}, which is much higher than that of pristine PU and PIM-1. The enhanced separation performance was derived from the shrunken interface voids after adding SBS. Blending PIM-1 with PU provides a new method for the modification of PIM-1.

Keywords: PIM-1 membrane; Polyurethane; Modification; Pervaporation

1. Introduction

Phenol is an important chemical raw material, which is mainly used in the production of caprolactam, salicylic acid, phenolic resin, and so on. During the production process of phenol, a large amount of phenolic wastewater arises. Therefore, the recovery of phenol from water will not only help to save the costs for factories, but also protects the aqueous environment [1]. The traditional methods of treating phenolic wastewater, such as adsorption, extraction, and distillation, are effective; however, they have limited feed concentration, and the problems of secondary pollution and adsorbent regeneration are associated with them [2].

Pervaporation (PV) is a novel separation technology that has been widely used in the separation of liquid solutions, in particular azeotropes, due to its simplicity, environmental friendliness, and energy-saving efficiency [3–5]. The suitable choice of membrane materials is the key to PV technology [6]. For the PV separation of phenol from water, some new membrane materials are being developed.

Significant attention has been paid to polymers of intrinsic microporosity (PIMs), which have high specific surface, controllable microporous structure, and excellent physical and chemical stability [7–10]. As a type of typical PIMs, PIM-1 derived from 5,5′,6,6′-tetrahydroxy-3,3,3′,3′-tetramethyl-1,1′-spirobisindane

* Corresponding author.

(TTSBI) and 2,3,5,6-tetrafluoroterephthalonitrile (DCTB) comprise fused ring sequences interrupted by sites of contortion. Thus, chains of PIM-1 cannot pack efficiently in the solid state and possess high free volume. PIM-1 has been widely researched in gas separation processes [11–13]. Recently, many researches have reported the potential of PIM-1 in organophilic PV to separate volatile organic compounds [14], alcohol [15], and phenol from water [16], among which the first publication is related to the recovery of phenol from water [17]. Budd et al. [16] used PIM-1 as a PV membrane to remove phenol from water and obtained separation factor of 18 and flux of 20.8 kg μm m^{-2} h^{-1}. PIM-1 membrane used in their research displayed a higher permeation flux than many other types of dense membranes, although the separation factor was moderate. In fact, PIM-1 has a structure rich in benzene rings and micropores, which benefits the separation of phenol. However, to the best of our knowledge, PV separation of phenol from water using PIM-1 membrane has not been reported by any other researcher. The applications of PIM-1 have not been exploited thoroughly. Based on this research situation, this study intended to develop the application of PIM-1 for phenol recovery from water.

To improve the performance of membranes, modification is necessary. The modification methods of PIM-1 membranes usually fall into two categories. On the one hand, it is based on the functionalization of nitrile group of PIM-1 backbone [18,19]. Carboxylation is usually carried out before further crosslinking or other treatment. Zhao et al. [20] prepared hydrolyzed PIM-1 membrane, and then used multivalent metal ions to carry out its crosslinking. Higher gas selectivity was obtained. On the other hand, second method involves the blending of PIM-1 with inorganic filler or other types of polymers, which seems to be more facile than group functionalization. Moreover, introduction of some required groups or components by mixing two or more materials together is relatively simple. Silicalite-1 [21], carbon nanotube [22], and graphene-like inorganic fillers [23] were added to PIM-1 to prepare mixed matrix membranes. Notably, the dispersion of these fillers is very important. Besides, PIM-1 (or carboxylated PIM-1) was also blended with polyimide [24], polyethylene [25], and polyetherimide [26]. The materials that are blended with PIM-1 should have particular affinity and benefit the separation of specific solvent. For example, Wu et al. [25] blended polyethylene with PIM-1, and the carbon dioxide (CO_2) selectivity of PIM-1 was remarkably enhanced. The effects of modification were related to the phase separation between PIM-1 and polyethylene.

For PV separation of phenol from water, polyether block amide (PEBA) [27], polydimethylsiloxane (PDMS) [28], and polyurethane (PU) [29] are usually selected as membrane materials. Among them, PU shows the highest separation factor; nonetheless, the permeability of PU is very limited. Das et al. and Ghosh et al. [30,31] prepared a series of hydrophobic hydroxyl-terminated polybutadiene (HTPB)-based PU membranes to remove phenol from water, and found that the separation factor was very high, even up to hundreds, but with a poor flux less than 0.01 kg m^{-2} h^{-1}.

Considering the combination of better permeability of PIM-1 and better selectivity of HTPB-based PU for the separation of phenol, the blending of PU and PIM-1 was considered to be feasible. Moreover, they not only have the complementary separation performances, but also capability of dissolution in co-solvent such as tetrahydrofuran and chloroform.

Therefore, in this study, PIM-1 and the modified PIM-1 membranes blended with HTPB-PU were prepared and characterized by optical microscopy (OM) and Fourier-transform infrared (FTIR) spectroscopy. Further, they were applied in the PV separation of phenol from water. Moreover, the effects of molecular weight of PIM-1, solvent used for membrane solution, content of PIM-1, and interface agent styrene–butadiene–styrene (SBS) on PV performance were investigated and discussed.

2. Experiment

2.1. Materials

The monomers TTSBI and DCTB were purchased from Sigma-Aldrich (Shanghai, China) and purified by re-crystallization and vacuum sublimation, respectively. Potassium carbonate (K_2CO_3) was obtained from Shanghai Chemical Reagent Store (Shanghai, China) and dried for 24 h under vacuum at 120°C. HTPB (hydroxyl value = 0.8355 mmol KOH g^{-1}) was purchased from Zibo Qilong Chemical Industry Co., Ltd. (Zibo, Shandong, China) and dehydrated under vacuum at 120°C with constant stirring for 2 h before being used. 1,4-Butanediol (BDO), dibutyltin dilaurate (DBTDL), tetrahydrofuran (THF), toluene, methanol, and chloroform were all supplied by Beijing Huihai Keyi Co., Ltd. (Beijing, China). BDO and THF were dried over molecular sieves (4 Å). Dimethylacetamide was purified by distillation under reduced pressure over calcium hydride and stored over molecular sieves (4 Å). 4,4′-Dicyclohexyl methane diisocyanate (H_{12}MDI, reagent grade, 90% isomers) was supplied by TCI (Shanghai, China) and employed without further purification. SBS (SBS1401, S/B of 20/80) was purchased from Yueyang Petrochemical (Hunan, China).

2.2. Preparation of PIM-1 and PU membranes

2.2.1. Preparation of PIM-1 membranes

The synthesis of PIM-1 was based on polycondensation of TTSBI and DCTB [32]. High-temperature polymerization procedure for PIM-1 is shown in Fig. 1(a). The yield of PIM-1 was approximately 92%. PIM-1 membrane was prepared by casting/solvent evaporation method. Membrane solution with 2 wt% was prepared by dissolving PIM-1 powder in chloroform. The solution was then filtered using 0.45 μm cut-off syringe filter and cast onto a Teflon holder with 9 cm diameter, so that the solvent could be evaporated slowly at room temperature. The dry membrane was formed after approximately 3 d, and further dried under vacuum at 80°C for 24 h. The yellow membrane with the thickness of about 40–80 μm was obtained. The molecular weight and molecular weight distribution were determined by gel permeation chromatography in THF.

2.2.2. Preparation of PU membranes

HTPB-PU was synthesized via two-step method including prepolymerization and chain-extension reactions as shown

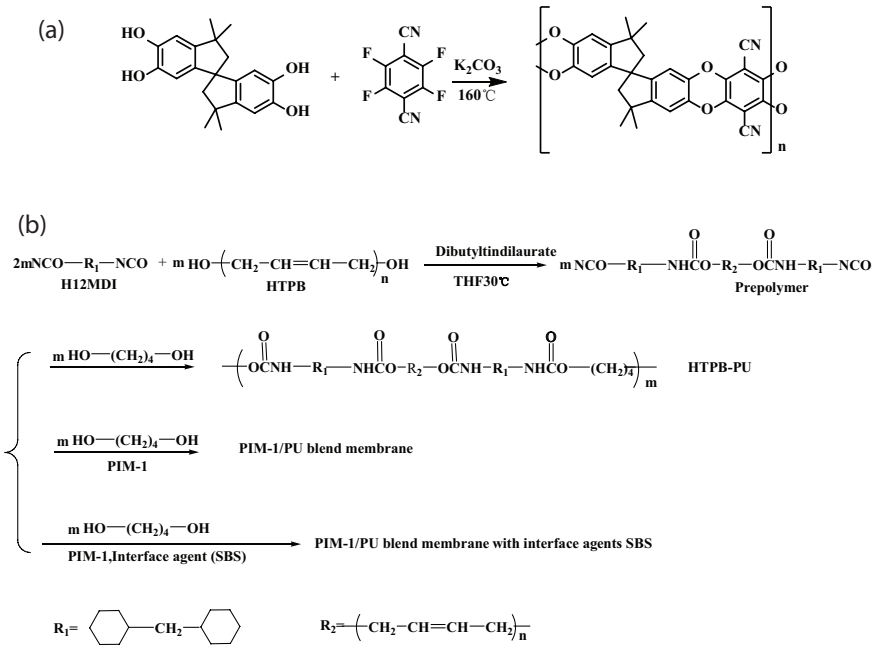

Fig. 1. Structures of PIM-1 and HTPB-PU: (a) PIM-1 and (b) HTPB-PU and blend membrane.

in Fig. 1(b) [1]. The prepolymer was prepared by the reaction of H_{12}MDI and HTPB in THF at 30°C for 1 h in the presence of 0.05 wt% DBTDL as catalyst with NCO/OH mole ratio of 2/1. Then, the chain-extender BDO (OH:NCO = 1:1) was added to the prepolyurethane under mechanical stirring for 15 min. Moreover, the solid content of solution was adjusted to about 15% by adding solvent. Finally, the membrane solution was cast on a Teflon holder and left at room temperature for 30 min, and then dried at 80°C for 10 h to remove the residual solvent. The thickness of the membranes was in the range of 80–150 μm.

2.3. Preparation of PIM-1/PU-blend membranes

PIM-1/PU-blend membranes were prepared by solution blending and casting. First, the prepolymer solution of PU was prepared according to the abovementioned procedure. Then, stoichiometric BDO and PIM-1 were added in the system for chain extension and blending. The following procedure was the same as that for the abovementioned preparation of PU membranes. For the preparation of PIM-1/PU-blend membranes with interface agent, SBS was added together with BDO and PIM-1 in the prepolymer of PU. The other procedures were similar to that for the preparation of PIM-1/PU-blend membranes without interface agent.

x%PIM-1/PU/y%(SBS) is used to designate PU membranes with x wt% PIM-1 and y wt% SBS loading. The PIM-1/z%PU represents PIM-1 membranes with z% PU blended. The solvents for preparing the membrane are abbreviated as C for chloroform and T for THF, which are presented in the parentheses following the designation of membranes. For example, PIM-1/1%PU(C) indicates PIM-1 membrane with 1% PU prepared in chloroform. For the blend membranes containing more PIM-1 than PU, chloroform was used as solvent for membrane solution; while for those with more PU than PIM-1, THF was used as solvent.

2.4. Membrane characterization

2.4.1. Fourier-transform infrared spectroscopy (FTIR)

The chemical composition of the membranes was determined by FTIR spectroscopy using a Nicolet IR 560 spectrometer (Thermo Nicolet Corporation, USA) measuring in the range of 4,000–500 cm^{-1}.

2.4.2. Optical microscopy

A microscope with integrated transmission/reflection light source from Shanghai Sunwell Optoelectronics Co., Ltd. was used to observe the membranes at different magnifications.

2.4.3. Thermogravimetric analysis

The thermal stability of the different types of membranes was tested using a TGA-2050 Simultaneous Thermal Analyzer (TA Instruments, USA). The temperature was in the range 30°C–800°C and the heating rate was 10°C min^{-1} with a nitrogen flow.

2.4.4. PV experiments

The PV performances of the membranes were tested by using an apparatus from Tiandabeiyang Co., Ltd. (Tianjin, China), as shown in Fig. 2. The feed was heated and circulated from the feed tank (volume of 1.5×10^{-3} m^3) through the upstream side of the membrane cell using a pump with adjustable function of flow rate. A membrane supported by porous sintered stainless steel in the permeate side was mounted in the PV cell. The measurements were carried out for phenol/water mixtures in which the content of phenol was 1–5 wt%. The feed mixture was maintained at a temperature between 50°C and 80°C using a thermostat. The effective

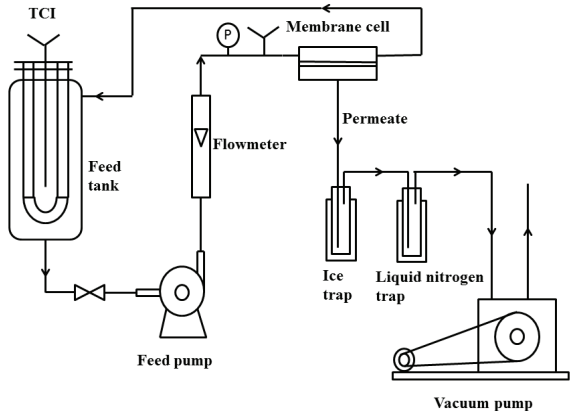

Fig. 2. Pervaporation apparatus.

area of the membrane was 2.2 × 10^{-3} m^2. Pressure on the permeate side was maintained below 200 Pa (absolute pressure) by vacuum pump. Two cold traps were set in parallel allowing the collection of permeate without rupture of the vacuum. The concentrations of permeate and feed mixture were analyzed by gas chromatography (GC). GC (GC1120 type, Sunny Optical Technology Company Limited, China) with thermal conductivity detector was used in this study. Packed column (OV-17, 3 m × 3 mm) was used for testing. When the permeate formed two-phase system, additional deionized water was added to dilute the permeate until a transparent solution of permeate was formed. Then, the as-obtained solution was injected into GC to test. The real concentration of original permeate could be calculated, because the amount of additional water was known. To avoid solidification of phenol on the pipe wall, the downstream pipe was wrapped with heated cable to maintain the temperature above 70°C.

The flux (J, kg μm m^{-2} h^{-1}), separation factor (α), and pervaporation separation index (PSI, kg μm m^{-2} h^{-1}) are defined by Eqs. (1)–(3) as follows:

$$J = \frac{Q}{A \cdot T} \cdot l \tag{1}$$

$$\alpha = \frac{Y_A \cdot X_B}{Y_B \cdot X_A} \tag{2}$$

$$\mathrm{PSI} = J \cdot (\alpha - 1) \tag{3}$$

where Q (kg) is the total mass of permeate collected through the effective area of the membrane (A, m^2) during time T (h), and l is the membrane thickness (μm). Y_A and Y_B represent the weight fractions of phenol and water in the downstream permeate, and X_A and X_B represent those in the feed mixture, respectively. PSI is introduced to evaluate the comprehensive separation performances of membranes considering permeation and selectivity together.

Permeability and selectivity are more representative and accurate than flux and separation factor, because permeability and selectivity decouple the effect of driving force. They are determined by using Eq. (4) [33] as follows:

$$P_i = \frac{J_i l}{x_{n,i} \gamma_i p_i^{\mathrm{sat}} - y_{n,i} p^p} \tag{4}$$

where P_i is the membrane permeability of the component i, l is the membrane thickness, p^p is the permeate pressure, $x_{n,i}$ and $y_{n,i}$ are the mole fractions of the component i in the feed and permeate, respectively, γ_i is the activity coefficient, and p_i^{sat} is the saturated vapor pressure. γ_i and p_i^{sat} are calculated by using the Wilson equation and Antoine equation, respectively.

The ideal membrane selectivity β is defined as the ratio of the permeability coefficients of component i relative to component j:

$$\beta = \frac{P_i}{P_j} \tag{5}$$

3. Results and discussion

3.1. Characterization of PIM-1 and PU modified PIM-1 membranes

3.1.1. FTIR spectra of membranes

Fig. 3 shows the FTIR spectra of the pristine and blended membranes. The spectra of PIM-1 and PIM-1/1%PU are similar and show characteristic peaks of PIM-1, which are nitrile (2,240 cm^{-1}), ether stretch (1,265 cm^{-1}), and aliphatic and aromatic C–H stretches (2,800–3,010 cm^{-1}) [32]. The characteristic peaks of PU can be observed in the spectrum of PU and 1%PIM-1/PU membranes as follows: 3,300 cm^{-1} (N–H stretching vibration), 1,642 cm^{-1} (C=O stretching vibration), and 970 cm^{-1} (C=C double bond of HTPB) [1]. The 1 wt% content of the additional blended polymer is so low that it cannot change the spectrum a lot.

3.1.2. Morphology characterization by OM

The PU/PIM-1-blend membranes exhibited a macroscopic phase separation in this study. Thus, optical microscope was used to observe the morphology of membranes from a larger scale. The as-prepared pure membranes such as PIM-1 and PU present uniform morphology appearance under light transmission as observed using optical microscope (Figs. 4(a) and (b)). Some gray shadows for PU were possibly induced by some air gaps between PU and base plate.

In contrast, the blend membranes exhibited a different morphology. PIM-1 showed a rigid backbone and limited flexibility. However, PU exhibited flexible soft segment of HTPB. Although both of them could be resolved in THF and chloroform, their difference in structure and properties could result in phase separation. Fig. 4(c) shows that 1 wt% PU seems to have relatively good compatibility with PIM-1, and no visible phase separation is observed. The possible reason is that the small amount of HTPB-based PU with flexible chain can penetrate into the micropores induced by the distorted structure of PIM-1. However, the blending of 1 wt% PIM-1 in PU induces obvious phase separation with yellow PIM-1 aggregates in PU matrix (Fig. 4(d)). PIM-1 has a tortile

structure and segment with weak mobility, which makes it difficult to diffuse into formed crosslinking net of PU domain. To increase the compatibility of PIM-1 and PU in 1%PIM-1/PU membrane, interface agent such as SBS was added in blend membranes based on similar compatible principle. The structure of styrene rich in benzene ring is similar to that of PIM-1, and that of butadiene in SBS is the same as soft segment of PU. Thus, SBS is an alternative interface agent for PIM/PU-blend polymer. Comparative analysis of the morphologies of samples with 0, 0.25, and 1 wt% SBS (Figs. 4(d)–(f)) indicates that PIM-1 agglomerates in 1%PIM-1/PU (Fig. 4(d)) tend to dissociate into smaller parts as shown in Fig. 4(e), and further spread all over the observed field of view (Fig. 4(f)) with the increase in the content of SBS. SBS, as interface agent, could exist between PIM-1 and PU. With the help of SBS, PIM-1 is not so repellent to PU, and becomes miscible with SBS. Thus, the original PIM-1 aggregates tend to disassemble into smaller parts, which are not excluded by PU for the existence of SBS. With increasing content of SBS, PIM-1 and PU become more compatible with each other as shown in Figs. 4(d)–(f).

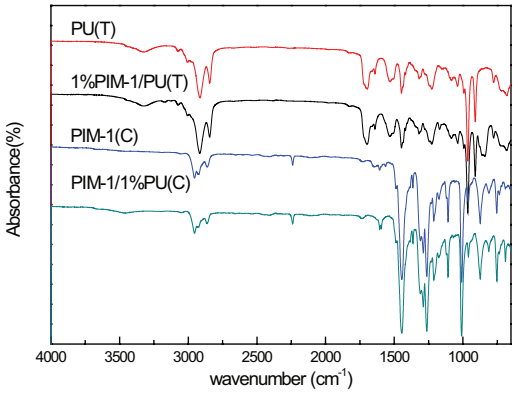

Fig. 3. FTIR spectra of membrane.

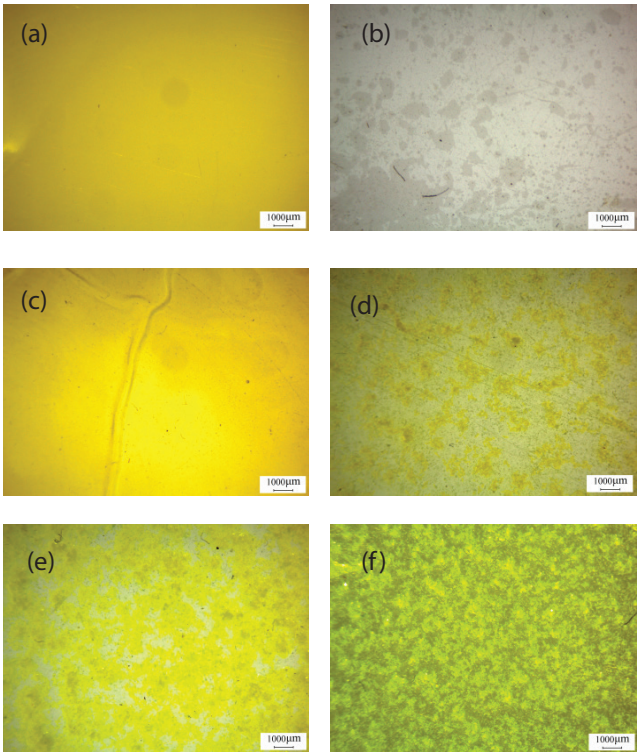

Fig. 4. Morphology of membranes by OM: (a) PIM-1(C), (b) PU(T), (c) PIM-1/1%PU(C), (d) 1%PIM-1/PU(T), (e) 1%PIM-1/PU/0.25%SBS, and (f) 1%PIM-1/PU/1%SBS.

3.1.3. Thermal properties of membranes

Fig. 5 shows TGA of PIM-1, PU, and blend membranes. The PIM-1 membrane shows a high decomposition temperature up to 500°C, which is estimated based on 4.5 wt% loss of the original weight, while that of PU is 250°C. Thus, the thermal stability of PIM-1 decreases slightly after adding 1 wt% PU. Similarly, the thermal stability of PU can be increased slightly by adding 1 wt% PIM-1. In this study, operating temperature of the PV was between 50°C–80°C. Thus, the thermal properties of these membranes could withstand the PV.

3.2. PV performance of membranes

3.2.1. Effect of molecular weight of PIM-1 on PV performances

The apparent and intrinsic separation performance of pristine PIM-1 membranes with different molecular weights was tested and calculated using 5 wt% aqueous phenol solution at 80°C as shown in Fig. 6. PSI keeps increasing with increasing molecular weight of PIM-1, which is due to the increased total flux and separation factor as evident in Fig. 6(a). Fig. 6(b) shows partial fluxes of phenol and water, indicating that phenol flux enhances gradually with increasing number-average molecular weight (Mn), while water flux increases to the maximum at Mn of 7×10^4 g mol^{-1} and then is restrained under higher Mn.

The membranes with different Mn were tested under the same feed temperature and concentration, thus permeabilities of solvents present a similar trend to partial flux according to Eq. (4). Selectivity increases with increasing Mn as shown in Fig. 6(c). The effects of Mn on separation performances can be explained in view of polymer structures. PIM-1 is a kind of porous polymer material, and longer molecule chains provide more micropores for solvents to diffuse.

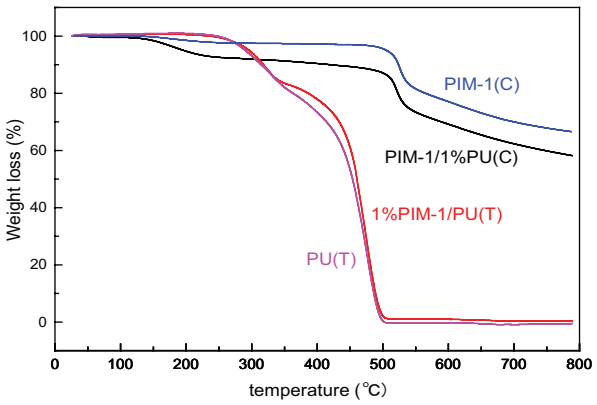

Fig. 5. TGA of membranes.

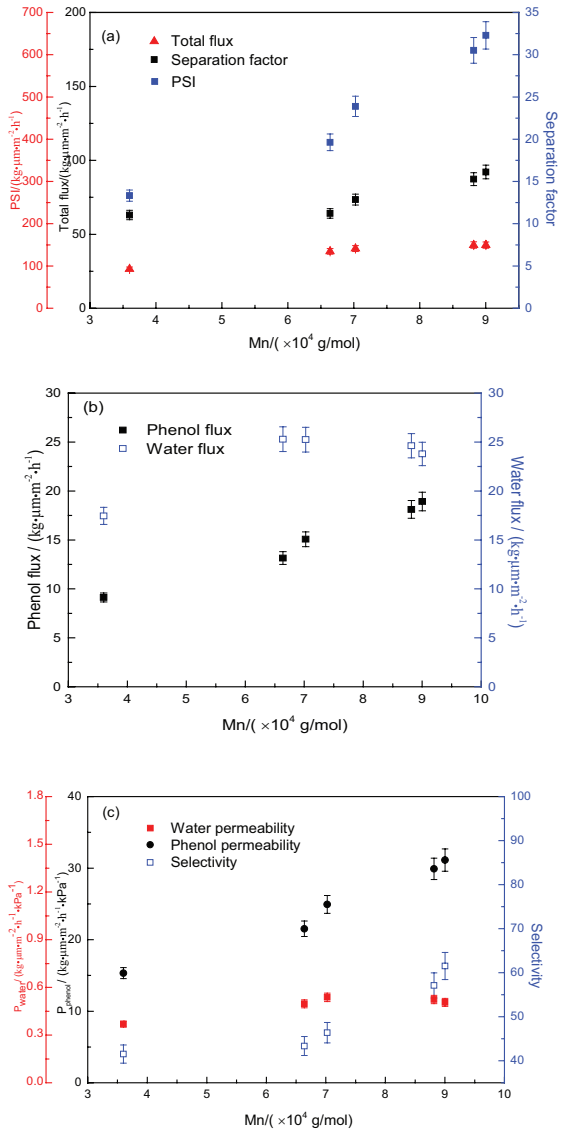

Fig. 6. Effects of molecular weight on separation performance: (a) total flux, separation factor, and PSI, (b) partial flux, and (c) permeability and selectivity (feed concentration: 5 wt% and temperature: 80°C).

Besides, kinetic diameter of phenol is about 5.1 Å [34], which is similar to the mean pore size of PIM-1 [16]. Thus, higher molecular weight results in higher phenol permeability and selectivity of PIM-1 membranes, which has been found by some studies [35]. Noteworthy, the permeability of water is much lower than that of phenol (Fig. 6(c)), while apparent flux of water is higher than that of phenol (Fig. 6(b)). This is attributed to lower driving force $(x_{n,i}y_i p_i^{sat} - x_{n,i}p^p)$ for phenol than water according to Eq. (4). PIM-1 membrane with Mn of 9 × 10⁴ g mol⁻¹ was selected for further study because of its good separation performance.

3.2.2. Effects of feed temperature and concentration

The effects of feed temperature and concentration on the PV performances of PIM-1 membrane were investigated. Fig. 7 shows the temperature dependence of performances of PIM-1 membranes with Mn of 9 × 10⁴ and 8.8 × 10⁴ g mol⁻¹, respectively. With increasing feed temperature, flux increases and separation factor slightly decreases (Fig. 7(a) for 8.8 × 10⁴ g mol⁻¹ and (b) for 9 × 10⁴ g mol⁻¹). That is a common phenomenon reported in many studies [36], which is usually ascribed to the enhanced movement of solvents and segments of polymer. Figs. 7(e) and (f) exhibit the intrinsic separation properties, revealing that both permeability and selectivity decrease with increasing temperature. This is mathematically attributed to a greater driving force at higher temperature induced by higher vapor pressure according to Eq. (4). In fact, that is the reason for desorption of water and phenol from membrane at higher temperature, although diffusion process is accelerated in membranes [33,37].

The abovementioned temperature dependence of partial flux and permeability can be plotted according to the Arrhenius equation [34] as follows:

$$J = J_0 \exp\left(\frac{-Ea}{RT}\right) \tag{6}$$

$$P = P_0 \exp\left(\frac{-E_P}{RT}\right) \tag{7}$$

where J_0 and P_0 are the pre-exponential factors, R is the universal gas constant, T is the operating temperature, and E_a and E_p are, respectively, the activation energies of flux and permeability which can be calculated. Based on the linear fitting of flux and permeability vs. temperature as shown in Figs. 7(c), (g), (d), (h), E_a and E_p can be calculated and the values are listed in Table 1. E_a and E_p are positive and negative values, respectively, which display the degree and direction of temperature effects on flux and permeability. Besides, PIM-1 (Mn = 9 × 10⁴ g mol⁻¹) obtains higher activation energy for water and lower one for phenol than PIM-1 (Mn = 8.8 × 10⁴ g mol⁻¹). This indicates that longer polymer chain can facilitate the diffusion of phenol and increase the energy barrier for water, which is in good agreement with the results presented in Fig. 6.

Feng and Huang [38] suggested that the difference between E_a and E_p was the molar enthalpy of vaporization ΔH_v expressed as follows:

$$\Delta H_v = E_a - E_p \tag{8}$$

Calculated values of ΔH_v of phenol and water are listed in Table 1. The values of ΔH_v are slightly different from theoretical values of 57.3 kJ mol⁻¹ for phenol [39] and 42.78 kJ mol⁻¹ for water [40] at 25°C under atmospheric pressure. That is probably induced by the prerequisite of Eq. (8) that the permeate pressure $y_{n,i}p^p$ is very low and neglected in derivation process.

Fig. 8 demonstrates that the feed content of phenol significantly affects the separation performances. The total flux and PSI increase, while the separation factor decreases gradually with increasing phenol concentration (Fig. 8(a)).

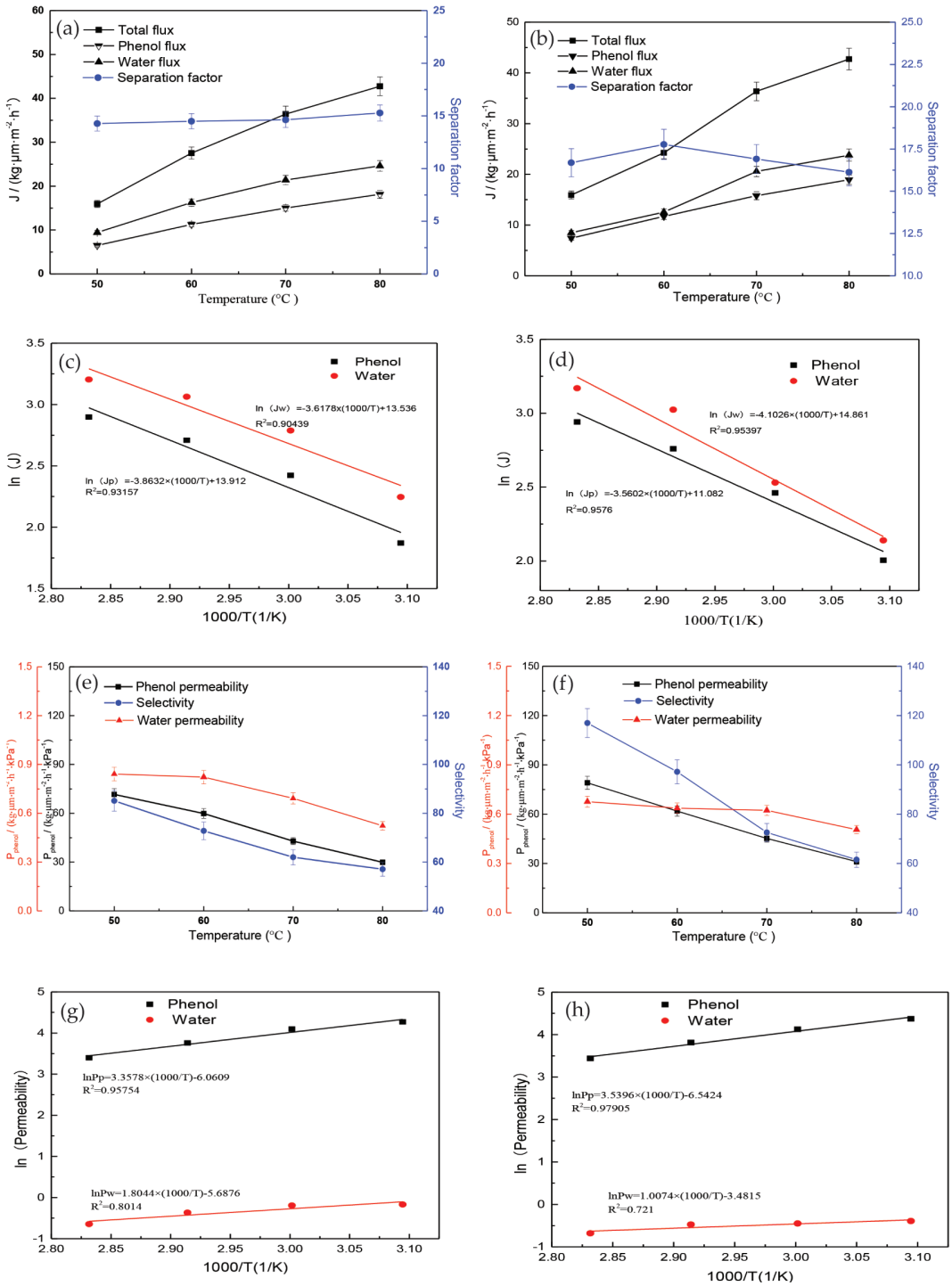

Fig. 7. Effects of feed temperature on separation properties: ((a) and (b)) flux and separation factor, ((c) and (d)) linear fitting of $1/T$ and Ln J, ((e) and (f)) permeability and selectivity, and ((g) and (h)) linear fitting of T and P (PIM-1 membranes: ((a), (c), (e), and (g)) Mn = 8.8 × 10^4 g mol^{-1}, ((b), (d), (f), and (h)): Mn = 9 × 10^4 g mol^{-1}, and feed concentration: 5 wt%).

Furthermore, the permeability and flux of phenol and water increase with the increase of feed content as shown in Figs. 8(b) and (c). Based on the hydrophobic nature of the PIM-1 membrane, the interaction between the membrane and phenol is higher than that of water and increases with increasing phenol concentration in the feed [41]. Thus, permeability of phenol increases. However, diffusion of water can also be facilitated because of more swelling of PIM-1 membrane under higher phenol concentration. The affinity of PIM-1 to phenol overwhelms the volume priority effect of water. Therefore, permeability of phenol increases faster than that of water, which induces increased intrinsic selectivity.

Table 1
Activation energies (kJ mol^{-1}) of solvents

$Mn_{(PIM-1)}$ (g mol^{-1})	8.8×10^4	9×10^4
$E_{a,water}$	30.08	34.11
$E_{a,phenol}$	32.12	29.6
$E_{p,water}$	–15	–8.38
$E_{p,phenol}$	–27.92	–29.43
$\Delta H_v = E_{a,water} - E_{p,water}$	45.08	42.49
$\Delta H_v = E_{a,phenol} - E_{p,phenol}$	60.04	59.03

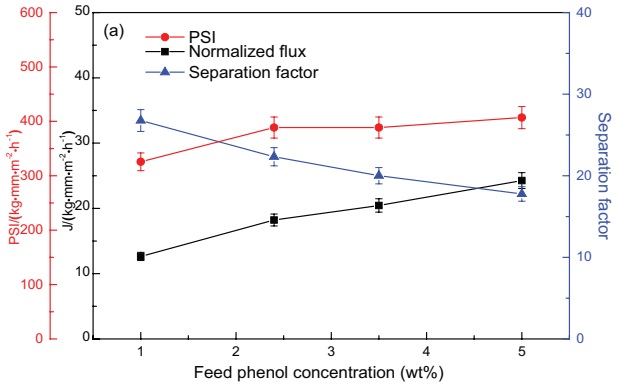

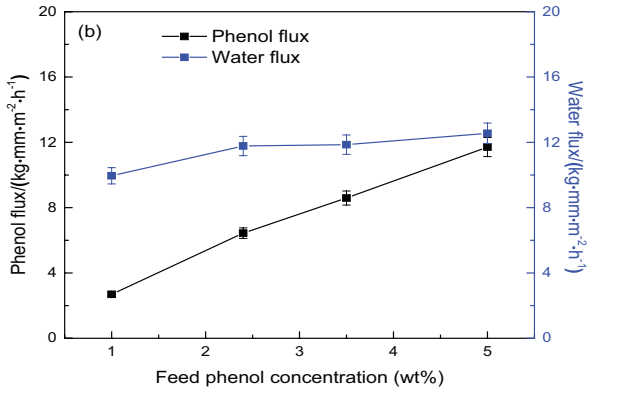

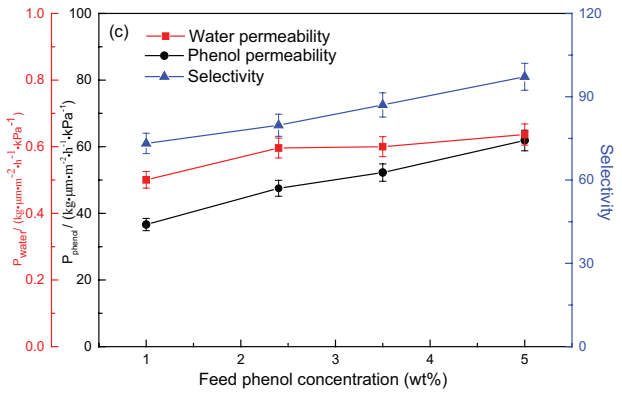

Fig. 8. Effects of feed concentration on separation performances: (a) total flux, separation factor, and PSI, (b) partial flux, and (c) permeability and selectivity (feed temperature 80°C and Mn = 9×10^4 g mol^{-1}).

3.2.3. Effect of blending modification on PV performance

Fig. 9 exhibits that the PV performance of pure PIM-1 and PU membranes is significantly influenced by solvents used in membranes solution. Chloroform and THF are suitable solvents for PIM-1 and PU to prepare membrane, respectively, obtaining relatively good separation performances. For example, the flux and separation factor of PIM-1(C) membrane prepared using chloroform are 12.6 kg μm m^{-2} h^{-1} and 26.8, while those of PIM-1(T) membrane obtained using THF as solvent are 44.9 kg μm m^{-2} h^{-1} and 3.3, respectively. Based on this result, chloroform was adopted as optimized solvent for preparing PIM-1/1%PU, and THF was used for 1%PIM-1/PU. The effects of solvent might have resulted from the packing of polymer chain.

Fig. 9(a) shows that the addition of 1 wt% PU in PIM-1 results in a decreased PSI compared with the pristine PIM-1 membranes. However, 1%PIM-1/PU(T) shows relatively good separation performance with total flux of 14.6 kg μm m^{-2} h^{-1} and separation factor of 21.7. PSI of 1%PIM-1/PU(T) is similar to that of PIM(C) and higher than that of the other membranes.

Fig. 9(b) demonstrates that the addition of 1% PIM-1 increases the phenol flux from 1.8 of PU(T) to 2.7 kg μm m^{-2} h^{-1} of 1%PIM-1/PU(T) and the water flux from 4.8 of PU(T) to 12.0 kg μm m^{-2} h^{-1} of 1%PIM-1/PU(T). Thus, 1%PIM-1/PU(T) achieves higher flux and lower separation factor than

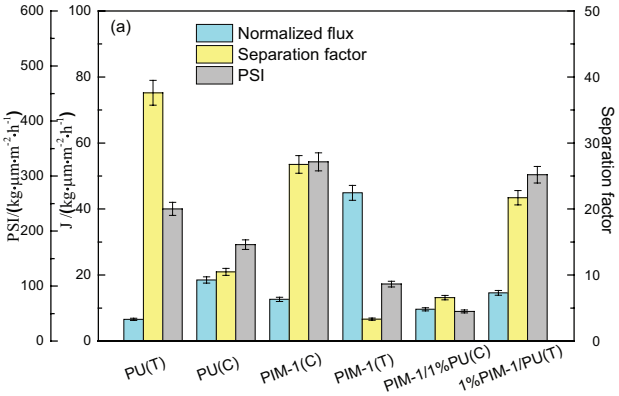

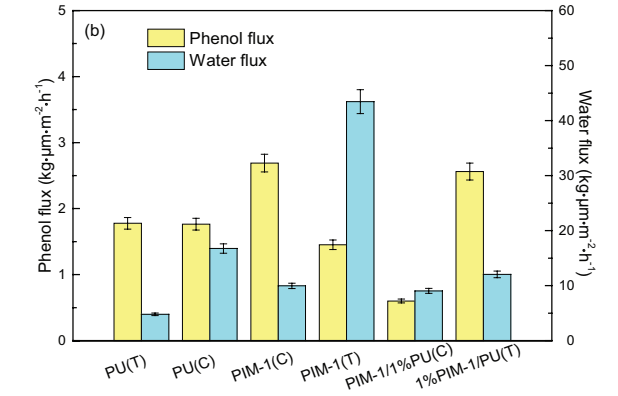

Fig. 9. Effects of blending modification on separation performances: (a) flux, separation factor, and PSI and (b) partial flux (phenol concentration: 1 wt%, temperature: 60°C, and Mn = 9×10^4 g mol^{-1}).

Table 2
Comparison of PIM-1, PU, and 1%PIM-1/PU

Membranes	Total flux (kg μm m^{-2} h^{-1})	Separation factor	PSI (kg μm m^{-2} h^{-1})	Cost[a] ($ kg^{-1})
PIM(C)	12.6	26.8	325.1	3107.0
PU(T)	6.6	37.6	240.3	14.5
1%PIM-1/PU(T)	14.6	21.7	302.2	45.4

[a]The cost of material is evaluated by the price from agent supplier listed in Section 2.1. The cost of solvents (THF or chloroform) is not taken into consideration, because they evaporate completely.

PU(T). In PIM-1/PU-blend membrane, small molecules diffuse through three paths: (1) PU domain, (2) PIM-1 domain, and (3) interface between PU and PIM-1. For 1%PIM-1/PU(T), the porous structure of PIM-1 remains in blend membrane because PIM-1 exists in the form of aggregates, thus paths between PIM-1 chains are available. Besides, the non-selective gaps induced by poor compatibility between PU and PIM-1 benefit the flux and limit the improvement of separation factor.

A comparison of separation performance and economical cost was made and summarized in Table 2. Although 1%PIM-1/PU(T) has similar PSI to PIM-1(C), the cost of 1%PIM-1/PU(T) of 45.4 $ kg^{-1} is much lower than that of PIM-1(C) of 3,107.0 $ kg^{-1}. Taking the economic efficiency of materials into consideration, 1%PIM-1/PU exhibits a promising future. Therefore, the effects of PIM-1 content on separation performance of PU were researched in the following study.

3.2.4. Effects of PIM-1 loading on separation performances

PIM-1/PU-blend membranes with different loading of PIM-1 were expected to have better performances and tested for PV separation as shown in Fig. 10. With the increase in loading of PIM-1 from 0.3 to 1.5 wt%, the flux keeps on increasing. However, separation factor first increases to the maximum at 1 wt%, and then decreases under higher loading. That is probably induced by poor compatibility between PIM-1 and PU. The interfacial void between PIM-1 and PU is nonselective and can facilitate the diffusion of water for the reason that molecular size of water is smaller than that of phenol. When PIM-1 with less than 1 wt% is added, the favorable factor of the microporous structure of PIM-1 with phenol affinity outweighs the unfavorable factor of the phase interface voids. However, at a higher PIM-1 loading above 1 wt%, the unfavorable factor plays a leading role to reduce the selectivity. Thus, improvement in the compatibility of two types of polymer becomes important, and the interfacial agents were added in this study for further investigation.

3.2.5. Effect of interfacial agent on PV performance

SBS was adopted as interface agent between PU and PIM-1 in this study. Fig. 11(a) demonstrates that with increasing SBS loading, the flux increases, which is mainly induced by the increased water flux shown in Fig. 11(b). The phenol flux increases first, and then decreases when the SBS content is higher than 0.125 wt%. This indicates that the separation factor increases to the maximum of 31.86 under loading of 0.125 wt% and then decreases gradually. A small amount of SBS as interfacial agent can narrow the gap between PIM-1 and PU. Therefore, water flux does not increase significantly

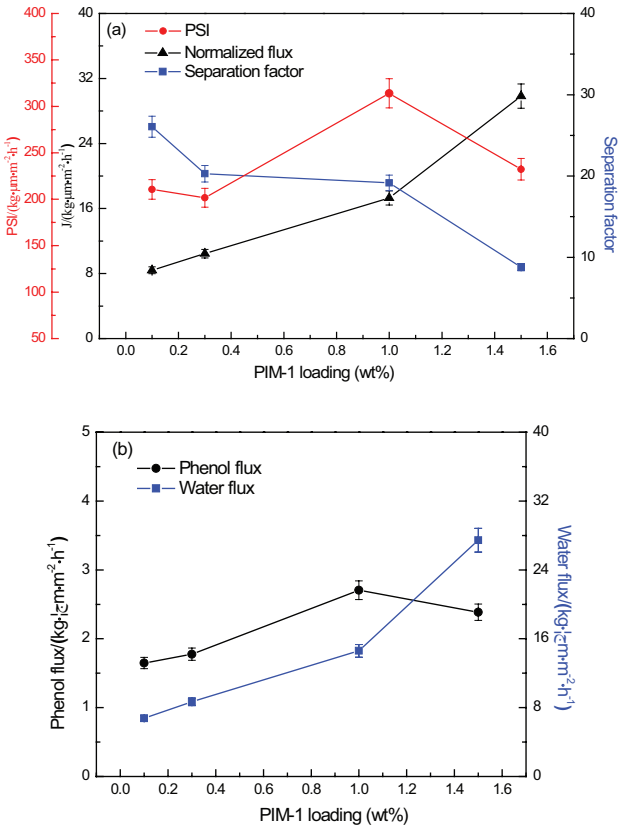

Fig. 10. Effects of PIM-1 loading on separation performances: (a) flux, separation factor, and PSI and (b) partial flux.

under SBS content lower than 0.5 wt% as shown in Fig. 11(b). However, SBS becomes an independent phase under higher loading and incompatible with PU and PIM-1, which facilitates the diffusion of water. Among these modified membranes with interfacial agent, the separation performance of 1%PIM-1/PU/0.125%SBS membrane was found to be the best with separation factor of 31.9, flux of 16.1 kg μm m^{-2} h^{-1}, and PSI of 498.1 kg μm m^{-2} h^{-1}. The synthetic performance of 1%PIM-1/PU/0.125%SBS was much higher than that of pure PIM-1 and PU membranes. Thus, SBS is an effective interfacial agent for the modification of blend membrane of PU/PIM-1.

3.2.6. Comparison with data reported in literature studies

The PV performance of PIM-1 and PIM/PU obtained in this study was compared with other types of membranes

Table 3
Comparison of pervaporation performance of different membranes

Membrane	Feed (wt%)	Temperature (°C)	Total flux (kg μm m^{-2} h^{-1})	Separation factor	PSI (kg μm m^{-2} h^{-1})	Reference
PDMS	1	70	15.0	7.6	113.8	[28]
HTPB-PU	3	70	2.7	62.8	166.9	[29]
PEBA2533	0.8	70	42.2	39.0	1,605.1	[36]
Polyimide	1	70	15.0	7.6	98.7	[42]
PIM-1	1	70	8.4	16.0	126.0	[16]
PIM-1(C)	1	60	12.6	26.8	325.7	This study
PIM-1(C)	5	70	42.7	16.1	646.0	This study
1%PIM-1/PU(T)	1	60	14.6	21.7	302.4	This study
1%PIM-1/PU/0.125%SBS	1	60	16.1	31.9	498.1	This study

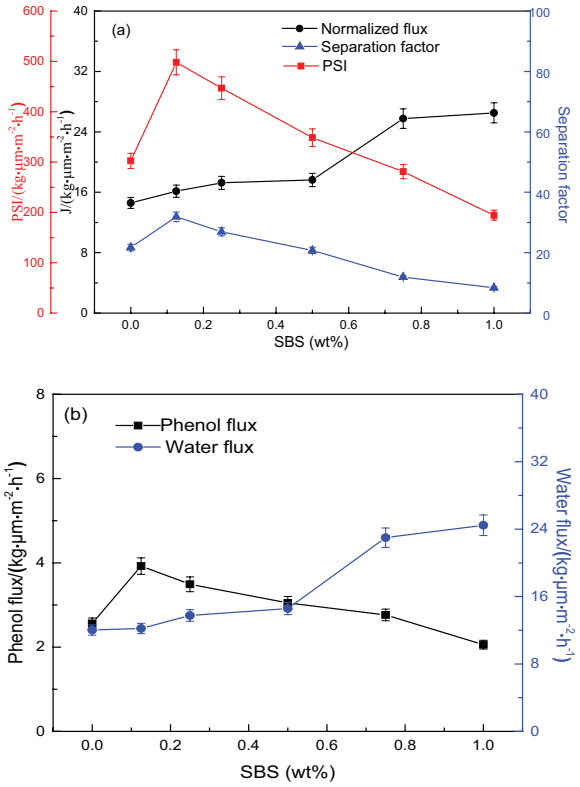

Fig. 11. Effects of SBS loading on separation performances: (a) total flux, separation factor, and PSI and (b) partial flux (feed temperature: 60°C, feed concentration: 1 wt%, and Mn = 12.8 × 10^4 g mol^{-1}).

discussed in literature reports as summarized in Table 3. Exact comparison of the separation performance under different test conditions was difficult. Notably, PSI can prove the potential of membranes in separating phenol from water to some extent. Table 3 summarizes that except for PEBA2533, PSI values obtained in this study are much higher than those obtained by other studies. PEBA possesses excellent comprehensive separation performance for recovery of phenol from water. Nonetheless, the casting process of PEBA membrane solution has to be carried out on a heated plate to avoid gelation [27]. Comparatively, the film-forming operation of PIM-1 and PIM-1-modified PU in this study can be conveniently conducted at room temperature. Table 3 summarizes that under 1% feed, PIM-1 membrane in this study achieves significantly higher flux, separation factor, and PSI at 60°C than PIM-1 from literature study [16] at 70°C. Higher feed temperature usually results in higher flux and lower separation factor. Thus, comparatively PIM-1 in our study performs better.

Hence, membranes obtained in this study are promising candidates for separating phenol from water.

4. Conclusions

PIM-1 and its blend membranes with PU were successfully prepared. PIM-1 with higher molecular weight leads to better PV separation performance. PU membrane modified with 1% PIM-1 shows higher PSI than pristine PU, and has similar PSI compared with pure PIM-1. Addition of SBS as interfacial agent can improve the separation performance of blend membrane. When 0.125 wt% of SBS is added to 1% PIM-1/PU-blend membrane, both total flux and separation factor increase simultaneously from 14.6 to 16.1 kg μm m^{-2} h^{-1} and from 21.7 to 31.9 with 1% phenol in feed at 60°C, respectively. PSI of 1% PIM-1/PU with 0.125 wt% SBS is 498.1 kg μm m^{-2} h^{-1}, which is much higher than that of pristine PU and PIM-1. The enhanced separation performance is derived from the shrunken interface voids after addition of SBS. Blending PIM-1 with PU and SBS provides a new method to improve the separation performance.

Acknowledgments

The authors gratefully acknowledge the financial support provided by the Beijing Natural Science Foundation (2172020), the National Key R&D Program of China (2017YFC1600605), Construction of technological innovation and service capability—Basic scientific research service fee-innovation platform of grain and oil food supply chain hazard identification and early warning technology (PXM2018_014213_000033), and National Natural Science Foundation of China (No. 21503007).

Symbols

PU	—	Polyurethane
PIMs	—	Polymers of intrinsic microporosity
SBS	—	Styrene–butadiene–styrene
x%PIM-1/PU/y%(SBS)	—	PU membranes with x wt% PIM-1 and y wt% SBS
PIM-1/z%PU	—	PIM-1 membranes with z% PU blended
C	—	Chloroform
T	—	Tetrahydrofuran
J	—	Total flux, kg μm m^{-2} h^{-1}
J_i	—	Partial flux of *i* component, kg μm m^{-2} h^{-1}
α	—	Separation factor
PSI	—	Pervaporation separation index
P_i	—	Permeability of *i* component, kg μm m^{-2} h^{-1} kPa^{-1}
$x_{n,i}$	—	Mole fraction of the component *i* in the feed
$y_{n,i}$	—	Mole fraction of the component *i* in the permeate
γ_i	—	Activity coefficient of *i* component
p_i^{sat}	—	Saturated vapor pressure, kPa
p^p	—	Permeate pressure, kPa
f_i	—	Fugacity of *i* component, kPa
β	—	Selectivity
E_a	—	Apparent activation energy of flux, kJ mol^{-1}
E_p	—	Permeability activation energies, kJ mol^{-1}
ΔH_v	—	Molar enthalpy of vaporization, kJ mol^{-1}

References

[1] H. Ye, Y. Wang, X. Zhang, Z. Zhang, B. Song, Polyurethane membrane with a cyclodextrin-modified carbon nanotube for pervaporation of phenol/water mixture, J. Polym. Eng., 37 (2017) 449–459.

[2] M.A. Hararah, K.A. Ibrahim, A.H. Al-Muhtaseb, R.I. Yousef, A. Abu-Surrah, A. Qatatsheh, Removal of phenol from aqueous solutions by adsorption onto polymeric adsorbents, J. Appl. Polym. Sci., 117 (2010) 1908–1913.

[3] H. Fan, Q. Shi, H. Yan, S. Ji, J. Dong, G. Zhang, Simultaneous spray self-assembly of highly loaded ZIF-8-PDMS nanohybrid membranes exhibiting exceptionally high biobutanol-permselective pervaporation, Angew. Chem. Int. Ed., 53 (2014) 5578–5582.

[4] G. Liu, W. Wei, W. Jin, Pervaporation membranes for biobutanol production, ACS Sustainable Chem. Eng., 2 (2014) 546–560.

[5] X. Lin, L. Xiong, G. Qi, Using butanol fermentation wastewater for biobutanol production after removal of inhibitory compounds by micro/mesoporous hyper-cross-linked polymeric adsorbent, ACS Sustainable Chem. Eng., 3 (2015) 702–709.

[6] H. Ye, X. Zhang, Z. Zhang, B. Song, W. Song, Application of polyurethane membrane with surface modified ZSM-5 for pervaporation of phenol/water mixture, J. Polym. Eng., 37 (2017) 777–784.

[7] P.M. Budd, B.S. Ghanem, S. Makhseed, N.B. McKeown, K.J. Msayib, C.E. Tattershall, Polymers of intrinsic microporosity (PIMs): robust, solution-processable, organic nanoporous materials, Chem. Commun., 2 (2004) 230–231.

[8] N.B. McKeown, P.M. Budd, Polymers of intrinsic microporosity (PIMs): organic materials for membrane separations, heterogeneous catalysis and hydrogen storage, Chem. Soc. Rev., 35 (2006) 675–683.

[9] N.B. McKeown, P.M. Budd, Exploitation of intrinsic microporosity in polymer-based materials, Macromolecules, 43 (2010) 5163–5176.

[10] N.B. McKeown, S. Hanif, K. Msayib, C.E. Tattershall, P.M. Budd, Porphyrin-based nanoporous network polymers, Chem. Commun., 23 (2002) 2782–2783.

[11] N. Du, M.M. Cin, I. Pinnau, A. Nicalek, G.P. Robertson, M.D. Guiver, Azide-based cross-linking of polymers of intrinsic microporosity (PIMs) for condensable gas separation, Macromol. Rapid Commun., 32 (2011) 631–636.

[12] P.M. Budd, K.J. Msayib, C.E. Tattershall, B.S. Ghanem, K.J. Reynolds, N.J. Mckeown, D. Fritsch, Gas separation membranes from polymers of intrinsic microporosity, J. Membr. Sci., 251 (2005) 263–269.

[13] S. Thomas, I. Pinnau, N. Du, M. Guiver, Hydrocarbon/hydrogen mixed-gas permeation properties of PIM-1, an amorphous microporous spirobisindane polymer, J. Membr. Sci., 338 (2009) 1–4.

[14] X.M. Wu, Q.G. Zhang, F. Soyekwo, Q.L. Liu, A.M. Zhu, Pervaporation removal of volatile organic compounds from aqueous solutions using the highly permeable PIM-1 membrane, AIChE J., 62 (2016) 842–851.

[15] S.V. Adymkanov, Y.P. Yampol'Skii, A.M. Polyakov, P.M. Budd, K.J. Reynolds, N.B. McKeown, K.J. Msayib, Pervaporation of alcohols through highly permeable PIM-1 polymer films, Polym. Sci. Ser. A Polym. Phys., 50 (2008) 444–450.

[16] P.M. Budd, E.S. Elabas, B.S. Ghanem, S. Makhseed, N.B. McKeown, K.J. Msayib, C.E. Tattershall, D. Wang, Solution-processed, organophilic membrane derived from a polymer of intrinsic microporosity, Adv. Mater., 16 (2004) 456–459.

[17] L. Gao, M. Alberto, P. Gorgojo, G. Szekely, P.M. Budd, High-flux PIM-1/PVDF thin film composite membranes for 1-butanol/water pervaporation, J. Membr. Sci., 529 (2017) 207–214.

[18] M.M. Khan, G. Bengtson, S. Shishatskiy, B.N. Gacal, Md.M. Rahman, S. Neumann, V. Filiz, V. Abetz, Cross-linking of polymer of intrinsic microporosity (PIM-1) via nitrene reaction and its effect on gas transport property, Eur. Polym. J., 49 (2013) 4157–4166.

[19] B. Satilmis, M.N. Alnajrani, P.M. Budd, Hydroxyalkylaminoalkylamide PIMs: selective adsorption by ethanolamine- and diethanolamine-modified PIM-1, Macromolecules, 48 (2015) 5663–5669.

[20] H. Zhao, Q. Xie, X. Ding, J. Chen, M. Hua, X. Tan, Y. Zhang, High performance post-modified polymers of intrinsic microporosity (PIM-1) membranes based on multivalent metal ions for gas separation, J. Membr. Sci., 514 (2016) 305–312.

[21] C.R. Mason, M.G. Buonomenna, G. Golemme, P.M. Budd, F. Galiano, A. Figoli, K. Friess, V. Hynek, New organophilic mixed matrix membranes derived from a polymer of intrinsic microporosity and silicalite-1, Polymer, 54 (2013) 2222–2230.

[22] M.M. Khan, V. Filiz, G. Bengtson, S. Shishatskiy, Md.M. Rahman, J. Lillepaerg, V. Abetz, Enhanced gas permeability by fabricating mixed matrix membranes of functionalized multiwalled carbon nanotubes and polymers of intrinsic microporosity (PIM), J. Membr. Sci., 436 (2013) 109–120.

[23] M. Alberto, J.M. Luque-Alled, L. Gao, M. Iliut, E. Prestat, L. Newman, S.J. Haigh, A. Vijayaraghavan, P.M. Budd, P. Gorgojo, Enhanced organophilic separations with mixed matrix membranes of polymers of intrinsic microporosity and graphene-like fillers, J. Membr. Sci., 526 (2017) 437–449.

[24] W.F. Yong, F.Y. Li, Y.C. Xiao, P. Li, K.P. Pramoda, Y.W. Tong, T.S. Chung, Molecular engineering of PIM-1/Matrimid blend membranes for gas separation, J. Membr. Sci., 407–408 (2012) 47–57.

[25] X.M. Wu, Q.G. Zhang, P.J. Lin, Y. Qu, A.M. Zhu, Q.L. Liu, Towards enhanced CO_2 selectivity of the PIM-1 membrane by blending with polyethylene glycol, J. Membr. Sci., 493 (2015) 147–155.

[26] L. Hao, J. Zuo, T.-S. Chung, Formation of defect-free polyetherimide/PIM-1 hollow fiber membranes for gas separation, AIChE J., 60 (2014) 3848–3858.

[27] W. Kujawski, A. Warszawski, W. Ratajczak, T. Porbski, W. Capała, I. Ostrowska, Application of pervaporation and adsorption to the phenol removal from wastewater, Sep. Purif. Technol., 40 (2004) 123–132.

[28] P. Wu, R.W. Field, R. England, B.J. Brisdon, A fundamental study of organofunctionalised PDMS membranes for the pervaporative recovery of phenolic compounds from aqueous streams, J. Membr. Sci., 190 (2001) 147–157.
[29] T. Gupta, N.C. Pradhan, B. Adhikari, Synthesis and performance of a novel polyurethaneurea as pervaporation membrane for the selective removal of phenol from industrial waste water, Bull. Mater. Sci., 25 (2002) 533–536.
[30] S. Das, A.K. Banthia, B. Adhikari, Porous polyurethane urea membranes for pervaporation separation of phenol and chlorophenols from water, Chem. Eng. J., 138 (2008) 215–223.
[31] U. Ghosh, N.C. Pradhan, B. Adhikari, Separation of water and o-chlorophenol by pervaporation using HTPB-based polyurethaneurea membranes and application of modified Maxwell-Stefan equation, J. Membr. Sci., 272 (2006) 93–102.
[32] B. Satilmis, P.M. Budd, Base-catalysed hydrolysis of PIM-1: amide versus carboxylate formation, RSC Adv., 4 (2014) 52189–52198.
[33] Y. Wang, T.S. Chung, B.W. Neo, M. Gruender, Processing and engineering of pervaporation dehydration of ethylene glycol via dual-layer polybenzimidazole (PBI)/polyetherimide (PEI) membranes, J. Membr. Sci., 378 (2011) 339–350.
[34] T. Atoguchi, T. Kanougi, T. Yamamoto, S. Yao, Phenol oxidation into catechol and hydroquinone over H-MFI, H-MOR, H-USY and H-BEA in the presence of ketone, Mol. Catal. A: Chem., 220 (2004) 183–187.
[35] G. Zhang, W. Gu, S. Ji, Z. Liu, Y. Peng, Z. Wang, Preparation of polyelectrolyte multilayer membranes by dynamic layer-by-layer process for pervaporation separation of alcohol/water mixtures, J. Membr. Sci., 280 (2006) 727–733.
[36] C. Ding, X. Zhang, C. Li, X. Hao, Y. Wang, G. Guan, ZIF-8 incorporated polyether block amide membrane for phenol permselective pervaporation with high efficiency, Sep. Purif. Technol., 166 (2016) 252–261.
[37] N.L. Le, Y. Wang, T.-S. Chung, Pebax/POSS mixed matrix membranes for ethanol recovery from aqueous solutions via pervaporation, J. Membr. Sci., 379 (2011) 174–183.
[38] X. Feng, R.Y.M. Huang, Estimation of activation energy for permeation in pervaporation processes, J. Membr. Sci., 118 (1996) 127–131.
[39] M.I. Yagofarov, R.N. Nagrimanov, B.N. Solomonov, Relationships between fusion, solution, vaporization and sublimation enthalpies of substituted phenols, J. Chem. Thermodyn., 105 (2017) 50–57.
[40] X. Wang, J. Chen, M. Fang, T. Wang, L. Yu, J. Li, ZIF-7/PDMS mixed matrix membranes for pervaporation recovery of butanol from aqueous solution, Sep. Purif. Technol., 163 (2016) 39–47.
[41] B. Sinha, U.K. Ghosh, N.C. Pradhan, B. Adhikari, Separation of phenol from aqueous solution by membrane pervaporation using modified polyurethaneurea membranes, J. Appl. Polym. Sci., 101 (2006) 1857–1865.
[42] F. Pithan, C. Staudt-Bickel, Crosslinked copolyimide membranes for phenol recovery from process water by pervaporation, ChemPhysChem, 4 (2003) 967–973.